Evaluation of chitosan composite beads for adsorption of gatifloxacin antibiotic compound from aqueous solutions

Joydeep Dutta (joydeep.dutta@lpu.co.in)
Lovely Professional University https://orcid.org/0000-0002-8183-5784
Aijaz Ahmad Mala
Lovely Professional University Faculty of Technology and Sciences
George D Kyzas
International Hellenic University - Kavala Campus: Diethnes Panepistemio tes Ellados - Panepistemioupole Kabalas

Research Article

Keywords: Adsorption, Antibiotics, Gatifloxacin, Chitosan, Walnut shell, Almond Shell

Posted Date: July 5th, 2022

DOI: https://doi.org/10.21203/rs.3.rs-1650426/v1

Abstract

In the present study, chitosan (C), walnut (W) and almond shell (A) powder were combined in different ratios to produce low-cost composite adsorbent beads for the removal of antibiotics gatifloxacin (GAT) from synthetic wastewater. The beads were characterized by a Scanning electron microscope, Fourier transforms infrared spectrum spectrophotometer and Energy-dispersive X-ray spectroscopy. The batch adsorption approach was employed to remove the antibiotic from the water. Moreover, isotherm and kinetics were conducted to illustrate the adsorption mechanism. Parameters like the effect of the adsorbent's dosage, pH, initial concentration and contact time on antibiotic adsorption were evaluated. Adsorption percentage increased slightly with the increase in adsorbent dosage. The optimum pH for GAT adsorption on beads was 5–7. In addition, adsorption increased with initial antibiotic concentration and time rise. The adsorption isotherm data were successfully fitted to Langmuir isotherm for AWC and CAW beads, while WAC beads followed the Freundlich isotherm. The highest adsorption was attained at pH 5 on CAW beads and pH 7 on AWC and WAC beads. The optimal contact time for equilibrium studies was 120 min for all types of beads. The adsorption isotherms data in AWC beads fit well with the Langmuir model and Freundlich adsorption for CAW and WAC beads. The rate of adsorption on beads follows Lagergren pseudo-second-order kinetics. The results indicate that prepared combination beads can be used to remove antibiotics from wastewater.

1. Introduction

Fluoroquinolones (FQs) are broad-spectrum antibiotics that have been extensively used as human and veterinary drugs (Wang and Wang 2019). Most FQs remain unmetabolized in human and animal bodies and are excreted (30–90%) with urine and faeces. They enter the aquatic bodies as unchanged or active forms (Mala and Dutta 2019; Patel et al. 2019; Ahmad and Dutta 2020). Conventional wastewater processes ineffectively remove them because of their bio-recalcitrance (Teglia et al. 2019). FQs antibiotics are detected in different water bodies, including surface water (He et al. 2015), groundwater (Du et al. 2014; Ma et al. 2015) and seawater (Zhang et al. 2013) systems.

Untreated F.Q.s antibiotic polluted wastewaters are toxic to microbes (Chao et al. 2014), inducing antibiotic resistance, troubled aquatic eco-complex systems and posing a severe threat to public health (Ahmad and Dutta 2018; Xiao et al. 2008).

Gatifloxacin (Fig. 1) belongs to FQ compounds and is used against gram-positive and gram-negative bacterial infections. It accounts for 17% of the world market, with a sale of USD$ 7.1 billion in 2009 (Dorival-Garcia et al. 2013). However, they have created severe cardiovascular toxicity to zebrafish (Shen et al. 2019) and will increase the risks to human health throughout the food chain. Furthermore, it has been reported to produce nausea, dizziness, headache, insomnia, agitation, and anxiety and cause the death of endothelial cells (Shen et al. 2019). Therefore, it must be either removed from the water or degraded. Thus, the effective treatment of antibiotic wastewater has become an essential issue (Chao et al. 2021).

Several processes to remove antibiotics have been studied, including nanofiltration, and reverse osmosis (Zularisam et al. 2006), electrochemistry (Carlesi et al. 2007), ozonation (Amouzgar and Salamatinia 2015), advanced oxidation (Garcia-Galan et al. 2016), membrane filtration (Balarak et al. 2016), advanced oxidation processes (Cheng et al 2016), biodegradation (Xiong et al. 2017), and photocatalytic degradation (Zhou et al. 2018). Unfortunately, most wastewater treatment technologies have low removal efficiency, costly and prolonged treatment time (Gonzalez-Pleiter et al. 2013; Garcia-Galan et al. 2016).

An alternative method like adsorption (Deng et al. 2011; Zeng et al. 2018) has been widely recognized as an effective, efficient and economical method for removal of water contaminants and removal of various antibiotic pollutants from an aqueous matrix because of its simple design, easy operation, flexibility and suitability for batch and continuous processes (Amouzgar and Salamatinia 2015; Chayid and Ahmed 2015; De Gisi et al. 2015; Ahmad and Dutta 2020). Adsorption is an attractive method for removing pollutants from wastewater because of its wide application range, environmental safety, easy operation and simple device. Adsorbents such as lotus stalk (Liu et al. 2011), date palm leaflets (El-Shafey et al. 2012), sawdust (Bajpai et al. 2012), biochars (Zheng et al. 2013), activated carbon (Ahmed et al. 2014; Nazari et al. 2016), chitosan (Vakili et al. 2015), cellulose (Rathod et al. 2015), paper towel (Xie et al. 2016), walnut shell (Yu et al. 2016), rice husk (Chen et al. 2016) and corn bracts (Yu et al. 2017) were used for the adsorption of antibiotics. However, high prices or low adsorption limit its feasibility. Nevertheless, an appropriate and efficient adsorbent is urgently needed.

Chitosan (a polysaccharide of *N*-acetyl-d-glucosamine and d-glucosamine) produced by the deacetylation of chitin is one of the natural polymers studied for the adsorption of pollutants due to the presence of amino groups, low cost, ease in availability. However, pure chitosan is weak at low pH swells and low adsorption capacity (Zhao et al. 2020). The activity of chitosan is improved by framing it into beads or sheet forms that can be easily removed from the water matrices and reused for adsorption. Agricultural wastes, separately or in combination with chitosan (Mala and Dutta 2021), are constantly being explored to develop competent composite adsorbents to frame mechanically stable systems as adsorbents. Plant residues have a porous and loose structure, and their surface contains abundant carboxyl, hydroxyl and other reactive groups (Wan et al. 2020). Reports have suggested that the lignin content of the plant residues can help in the immobilization of antibiotic tetracycline and ciprofloxacin (Nazari et al. 2016). Hence, they can be used as efficient adsorbent materials. Walnut shell is used as an adsorbent for the removal of cephalexin antibiotic (Nazari et al. 2016), tetracycline and sulfamethoxazole (Popoola 2020), cefixime (Ahmad and Dutta 2020) and Gemifloxacin (Mala and Dutta 2021). Almond shells are low-cost, renewable and environmentally-friendly materials for water treatment. Almond shells can adsorb antibiotics like amoxicillin (Homem et al. 2010; Homem et al 2015; Flores-Cano et al. 2016), metronidazole and dimetridazole (Flores-Cano et al. 2016), cefixime (Ahmad and Dutta 2020) and Gemifloxacin (Mala and Dutta 2021). Therefore, the study focused on developing chitosan-based composite hydrogel beads using plant residues.

The present study aims to prepare and characterize composite beads using (chitosan, walnut, and/or almond shell) in different proportion to remove gatifloxacin from water. The adsorption kinetics, isotherms and adsorption mechanisms were studied in detail. Furthermore, the experimental adsorption factors such as contact time, pH, initial concentration and adsorbent dosage were also analyzed.

2. Materials And Methods

2.1. Materials and reagents

Gatifloxacin antibiotic (Fig. 1) (99%) was purchased from Yarrow Chemicals (India). Acetic acid, sodium hydroxide, and glutaraldehyde were purchased from the Loba Chemie reagent Company. Ltd (India). Chitosan powder (high-molecular-weight) was purchased from Himedia (India). Walnut and almond shells were collected from local markets.

2.2. Adsorbent preparation

Walnut and almond shells were washed twice in distilled water to remove the dust, dried at 105ºC for 24 h, then ground and sieved separately to obtain a powder of adsorbent particles. Chitosan was used without any further purification. Chitosan (C), walnut (W) and almond shell (A) powder adsorbents (in different combinations as almond shell:walnut: chitosan 2:1:1 (AWC), chitosan: almond shell: walnut 2:1:1 (CAW), and walnut: almond shell: chitosan 2:1:1 (WAC)) dissolved in glacial acetic acid (2.0%). The solutions were agitated by a magnetic stirrer (8–10 h) at room temperature (30 ± 2°C). Then the mixed solution is released dropwise into a NaOH (0.5M) with a syringe to form spherical beads. The beads were kept for 16 h in NaOH (0.5M) for imbibition. The beads (1.5 g) at pH 5 were treated with 15 mL glutaraldehyde solution (2.5%) for activation purposes. The beads were stirred at 150 rpm for 3 hrs. (room temperature). Then, the activated beads were washed to remove unreacted glutaraldehyde until a neutral pH was obtained and finally dried in an air oven at 50 ºC for 24 h. The final materials were stored in air tight bottles for further use.

2.3. Adsorption experiments

2.3.1 Effect of the initial pH

Batch experiments studied the effect of the initial pH. 0.1 g of the samples were inserted into 50 mL of GAT solution (C_0 = 30 mg/L) in a conical flask. The adjustment of solution pH (at pH = 3, 5, 7, 9, 11) was conducted with micro-additions of HCl (0.01 M) or NaOH (0.01 M) aqueous solutions. Using a shaking bath, the flasks were allowed to agitate (N = 50 rpm) at 30 ℃ for 24 h. Finally, the residual GAT concentration analysis was carried out. All experiments were conducted in triplicates.

2.3.2 Isotherms

A weighted amount of the samples (0.1 g) was inserted into a conical flask which contained 50 mL of GAT solution of different initial concentrations (C_0 = 10–50 mg/L) at an initial pH of 7 since the optimum value of the initial pH was found to be 7 (from section 2.3.1). The adjustment of initial pH was achieved with micro-additions of HCl solution (0.01 M) or NaOH (0.01 M). Then, the flasks were shaken for 24 hr at 30 ℃ with a fixed agitation speed (150 rpm) using a shaking bath.

2.3.3 Effect of contact time

A weighted amount of the samples (0.1 g) was inserted into a conical flask which contained 50 mL of GAT solution of initial concentrations (C_0 = 30 mg/L) at an initial pH of 7 since the optimum value of the initial pH was found to be 7 (from section 2.3.1). The adjustment of initial pH was achieved with micro-additions of HCl solution (0.01 M) or NaOH (0.01 M). Then, the flasks were allowed to be shaken at 30 ℃ with a fixed agitation speed (150 rpm) using a shaking bath. The residual concentrations of ions were analyzed at predefined time intervals (30, 60, 90, 120, 150, and 180 mins). Moreover, the calculations of residual concentrations of ion (C_e) in the liquid phase were achieved according to the above section 'pH-effect'.

2.3.4 Effect of adsorbent's dosage

A weighted amount of the samples (0.1-1.0 g) was inserted into a conical flask which contained 50 mL of GAT solution of initial concentrations (C_0 = 30 mg/L) at an initial pH of 7 since the optimum value of the initial pH was found to be 7 (from section 2.3.1). The adjustment of initial pH was achieved with micro-additions of HCl solution (0.01 M) or NaOH (0.01 M). Then, the flasks were allowed to be shaken for 24 h at 30℃ with a fixed agitation speed (150 rpm) using a shaking bath. The residual concentrations of ions were then analyzed.

2.3.5 Analysis and modelling

The residual GAT concentration was evaluated using a U.V. spectrophotometer (U-2000, Hitachi, Japan). The U.V. absorbance was adjusted at λ_{max} = 263 nm. The absorbance wavelength change was calculated from the obtained results, revealing an absorbance maximum change of ~ 2%, and hence was determined as unimportant. The design of calibration curves from absorbance versus GAT concentration was achieved using the linear relationship of Beer-Lambert. In addition, using the equation of mass balance, as depicted below (Eq. (1)), was calculated the GAT amount which removed due to equilibrium phase Q_e (mg/g), where C_0 and C_e (mg/L) are mentioned in the initial and equilibrium concentrations of GAT, respectively; V (L) is the aqueous solution volume; m (g) is the mass used.

$$Q_e = \frac{(C_0 - C_e)V}{m} \quad (1)$$

2.4. Characterization techniques

The morphology of the beads was analyzed by a Scanning electron microscope (SEM-JEOL 6100). Fourier transform infrared spectrum (FT-IR) spectrophotometer (Shimadzu-8400) was applied in the range 4000 – 450^{-1}cm at room temperature to reveal the groups functionalized onto the adsorbent's beads surface. The elemental composition of surfaces was analyzed by Energy-dispersive X-ray spectroscopy (EDX).

3. Results And Discussion

3.1. Characterization of beads

Chitosan received great interest due to its cationic groups, high adsorption capacity, molecular structure, biodegradability, abundance and low cost. However, due to the protonation of free amino groups, the polymer is fully soluble below pH ~5 (Crini and Badot 2008), low mechanical strength and low surface area (Vakili et al. 2015), thus limiting its capability of sorbate binding (Filipkowska and Jozwiak 2013). The latter can be overcome by modifying chitosan to increase its mechanical strength and adsorption capacity. Lignin, cellulose and hemicellulose are integral parts of the plant cell and provide mechanical strength. Almond and walnut shells were a choice of composite materials as the chemical composition (Table 1) of the shells provides the required mechanical strength to the beads as adsorbents. The chemical composition of shells varies: Walnut shells had 36.38% cellulose, 27.85% hemicellulose and 43.7 % lignin; Almond shells had 38.47% cellulose, 28.82% hemicellulose and 29.54% lignin.

Table 1
Proportion of cellulose, hemicellulose, lignin

Material	Cellulose (wt. %)	Hemicellulose (wt. %)	Lignin (wt. %)
Walnut shells	36.38	27.85	43.70
Almond shells	38.47	28.82	29.54

Scanning electron micrographs present the surface morphology of synthesized beads before and after adsorption. Before adsorption, the AWC beads (Fig. 2a) showed an irregular appearance with different gradients of scattered fissures and occasional pores. After adsorption (Fig. 2b), the SEM image was layered with fair surface topography and resembled clouds of an overcast sky. In the case of CAW beads (Fig. 2c), the SEM image showed multiple layers with the formation of chunks of varying sizes, fissures and conspicuous pores. The post-processed image (Fig. 2d) showed that the structure formed has reduced in size and adhesion pattern, indicating an activity. The WAC beads' surface seems rough and multiplies layered, giving an uneven outlook (Fig. 2e). After adsorption, the post-processed SEM image (Fig. 2f) showed that agglomerates became more condensed and tightly packed. A dispersive energy spectrum (EDX) showed that the beads contain a maximum carbon component followed by oxygen (Ahmad and Dutta 2020).

The FTIR spectra for the beads were taken in the range 450–4000 cm^{-1}, which was performed to distinguish functional groups present on the outside of the adsorbent that can conceivably support the adsorption of anti-infection agents as shown; it can be shown in Fig. 3, N–H, OH and C = O groups were found on the prepared beads, which are considered as a decent decision for adsorption measure (Kumar et al. 2018).

The C–H bonds at 3700–3800 cm^{-1} indicate the presence of alkenes or aromatic compounds, while the peaks at 3273, 3255 and 3288 cm^{-1}indicate hydrogen bonding (O–H) stretch, suggesting the presence of phenols and alcohols in AWC (Fig. 3a), CAW (Fig. 3b) and WAC (Fig. 3c) beads. The sharp peaks at 2359, 2362 and 2355 cm^{-1} confirm the presence of the N–H group for amino groups. When response happens between aldehyde groups of glutaraldehyde and some amino groups of beads, the amine groups may be formed (Migneault et al. 2004). The peaks support the transformation at 1643, 1647 and 1649 cm^{-1}(C = O stretch). After adsorption, the pinnacles have gotten limited in the event of AWC (a) beads. The pinnacles got heightened after adsorption if there should be an occurrence of CAW (b) beads. There was a minimal extensive distinction between them when adsorption tops on WAC (c) beads. It was observed that the interaction was due to hydrogen bonding between hydroxyl of alkali lignin with β-1, 4- glycosidic linkage of chitosan and alkyl-substituted ether of alkali lignin with the hydroxyl group of chitosan. There was no significant change in the peaks of primary amine, confirming no involvement of primary amine of chitosan in composite formation (Nair et al. 2014).

3.2. Effect of pH and adsorption mechanism

The pH of the solution is an important parameter affecting the adsorption of any pollutant, as it can influence the physiochemical properties, surface binding sites and charge of both adsorbents (Ahsan et al. 2018; Yadav et al. 2018) and adsorbate (Seo et al. 2017). Therefore, the adsorption efficiencies of beads were studied at different pH values (3–11) with the fixed initial concentration of antibiotics (30 mg/L) and contact time of 180 min. At lower pH values, the amino groups of FQs get protonated (Amin et al. 2007), and at higher pH values, they behave as anions due to the deprotonation of carboxylic groups. However, at neutral pH, zwitterion exists (Yadav et al. 2018); hence, the study was spread over a range from pH 3–11.

The carboxylic groups present in the GAT molecules get ionized to yield – COO- groups while –NH groups of the piperazine ring get protonated to $–NH2^{+}$ when the drug is in its solution form of pH 5–7. The adsorption of GAT onto the beads is due to the interaction between the above-charged species with the charges on the beads. The chitosan composite beads grafted with plant materials like almond and walnut added lignin, cellulose and hemicellulose adsorption are mainly due to electrostatic attraction between negative moiety (COO-) of GAT and $NH3^{+}$ of composite, polar π–π stacking dipole-dipole interplays with the cellulose and lignin fractions with GAT at pH 5–7. Maximum adsorption of gatifloxacin at pH 5.0 on CAW (85%). A similar observation was reported in other studies, in which the amoxicillin adsorption increases from pH 2 to 5 as the carboxyl functional groups (–COOH) on the amoxicillin readily dissociate to carboxylate ($–COO^{-}$) ions, thus increasing the electrostatic attraction between amoxicillin and the adsorbent (Putra et al. 2009; Moussavi et al. 2013). The adsorption of GAT was maximized at pH 7.0 on AWC (84%) and WAC (82%) beads, respectively (zwitterionic form), which may be due to the protonated amino groups that still can favour the adsorption (Yadav et al. 2018). In even higher pH values, the decrease in the adsorption was attributed to the deprotonation of C = O groups on antibiotics and beads, which significantly caused electrostatic repulsion between negatively charged groups of beads and antibiotics (Jiang et al. 2013). WAC beads followed a lower adsorption level onto its surface than the other two compositions (Fig. 4). The FTIR analysis shows that all three

different beads contain –O.H., and C = O groups, which give negative charges due to the oxygen-containing groups (Yadav et al. 2018). Studies have reported that the maximum removal of different antibiotics found to be optimum at a pH range from 5.0–7.0, like norfloxacin (Feng et al. 2018) Tetracycline (Fan et al. 2018), sulfamethoxazole (Soares et al. 2019), levofloxacin (Mahmoud et al. 2020) and ciprofloxacin (Fu et al. 2021).

3.3. Effect of adsorbent's dosage

The removal of antibiotics was improved with the increase in adsorbent dose. The uptake value increases almost linearly as the adsorbent amount rises from 0.1 to 1.0 g. The increase was from 81 to 88% by AWC beads, 80 to 88% by CAW beads and 81 to 88% by WAC beads when the adsorbent dosage increased from 0.1 to1.0 g (Fig. 5a). This behavior was attributed to the increasing number of active sites, which causes the attraction of more antibiotic molecules on the bead's surface (Kakavandi et al. 2014; Chen et al. 2014; Ahsan et al. 2018) When the adsorbent dosage increased from 0.1 to 1 g/L, the gatifloxacin adsorption percentage increased slightly. Therefore, it can be concluded that 0.1 g as the adsorbent's dosage was adequate because only a slight increase was presented (~ 7% increase) for all beads. However, the removal value decreases non- significantly for AWC beads, which later made up to the maximum value as other combinations. An increase in adsorbent dosage causes adsorption of ciprofloxacin (Danalıoğlu et al. 2017; Liang et al. 2018), tetracycline and chlortetracycline (Ma et al. 2019). In another study (adsorption of cephalexin onto walnut shell-based activated carbon), it was found that the adsorption capacity decreased considerably with the increase of adsorbent dose (Nazari et al. 2016).

3.4. Effect of initial concentration

The rate of adsorption is a function of the initial concentration of the adsorbate, which is an essential factor for effective adsorption. The effect of initial concentrations of adsorbed antibiotics onto beads is presented in Fig. 6. The removal of antibiotics was found to decrease with the increase of antibiotic concentration. In the case of AWC beads, the adsorption decreased from 96 to 63% with the rise of initial GAT concentration, while the adsorption decreased from 96 to 65% and 94 to 62% in the case of CAW and WAC beads, respectively. This can be explained by considering that all adsorbents have a fixed/limited number of active adsorption sites. The active sites become saturated under the same experimental conditions (Balarak et al. 2016). The results obtained in this study are in agreement with a decrease in the adsorption percentage of antibiotics like cephalexin (Khosravi et al. 2018), norfloxacin (Feng et al. 2015), ciprofloxacin (Fu et al. 2021) and—chlortetracycline antibiotic (Tunc et al. 2020) with their increase in initial concentration respectively.

For the isotherm modelling, Langmuir (Eqs. (2, 4)) and Freundlich (Eq. (3, 5)) (Ahmed and Theydan 2014) isotherm equations were used for fitting adsorption equilibrium data (in non-linear and linear form), and the following equations illustrate them:

$$\frac{C_e}{Q_e} = \left(\frac{1}{Q_m}\right)C_e + \frac{1}{K_L Q_m} \quad \text{(Linear form of Langmuir equation) (2)}$$

$$\log\left(Q_e\right) = \frac{1}{n}\log\left(C_e\right) + \log\left(K_F\right) \quad \text{(Linear form of Freundlich equation) (3)}$$

$$Q_e = \frac{Q_m K_L C_e}{1 + K_L C_e} \quad \text{(Non-linear form of Langmuir equation) (4)}$$

$$Q_e = K_F C_e^{1/n} \quad \text{(Non-linear form of Freundlich equation)} \qquad (5)$$

where Q_m (mg/g) is the maximum amount of adsorption; K_L. (L/mg) is the Langmuir constant of adsorption equilibrium; K_F ($mg^{1-1/n}\ L^{1/n}/g$) is the Freundlich constant which symbolizes the capacity of adsorption; n is the constant that represents the intensity of adsorption (dimensionless).

All the values of constants for the isotherms were compiled in Table 2. The data were analyzed to see whether the isotherm obeyed Langmuir and Freundlich isotherm model. Adsorption was considered satisfactory when the Freundlich constant n values were between 1–10 (Deng et al. 2011). The adsorption of gatifloxacin on chitosan and almond/ walnut composite beads and its equilibrium data were fitted to the Langmuir and Freundlich isotherms. The R^2 calculated by Langmuir was the highest in ACW beads than the Freundlich equation. Therefore, Langmuir was the best fit for isotherm for gatifloxacin adsorption on ACW beads which showed the surfaces of these materials had nearly homogenous sites for gatifloxacin adsorption. Furthermore, the maximum monolayer coverage capacity (Q_m) calculated by the Langmuir isotherm was obtained (35.84 ± 0.49 mg/g), and K_L 0.45 L/mg and R^2value are 0.999 showing sorption fitted to the Langmuir model of gatifloxacin on ACW beads.

Table 2
Isothermal parameters for the adsorption of gatifloxacin antibiotic compound on AWC, WAC, CAW.

	Langmuir equation			Freundlich equation		
	Q_m	K_L	R^2	K_F	n	R^2
Material	mg/g	L/mg		$mg^{1-1/n}\ L^{1/n}\ g^{-1}$		
ACW	35.84 ± 0.49	0.45 ± 0.02	0.999	12.63 ± 1.93	2.90 ± 0.55	0.949
CAW	35.81 ± 0.48	0.47 ± 0.03	0.996	14.69 ± 0.56	3.39 ± 0.19	0.995
WAC	34.22 ± 1.82	0.48 ± 0.10	0.983	13.03 ± 0.77	3.14 ± 0.25	0.991

3.5. Effect of contact time

The effect of contact time on the adsorption of GAT is a function of time, as shown in Fig. 7. Initially, the antibiotic removal rate is higher, but it becomes slow as it reaches equilibrium (plateau). Similar results were obtained when amoxicillin was adsorbed onto the almond shell (Homem et al. 2015). The graph depicts that the adsorption percentage reached 84%, 88%, and 88% in 180 minutes for AWC, CAW, and WAC beads. The high availability may explain the high adsorption rate at the initial stage in the number of active binding sites on the adsorbent surface, which gradually is occupied by the antibiotic molecules and tends to become almost constant. Similar results were obtained in the adsorption of tetracycline and sulfamethoxazole onto nanomagnetic walnut shell-rice husk (Popoola 2020). After a definite time, the empty sites are challenging to be covered due to the repulsive forces between solute molecules available in the solid and bulk phase. The adsorption is likely an attraction-controlled process in the later stage due to fewer available sorption sites (Azarpira and Balarak 2016). As the surface adsorption sites become exhausted, the uptake rate is controlled by the rate at which the adsorbate is transported from the exterior to the interior sites of the adsorbent particles. Gatifloxacin adsorption on all the combination beads shows maximum adsorption at 120 mins, followed by a plateau phase. This study is in agreement with the adsorption of tetracycline and chlortetracycline on chitosan (Liang et al. 2018), Ciprofloxacin and enrofloxacin antibiotics adsorption onto chitosan hydrogels (Wang et al. 2019), and chlortetracycline adsorption on chitin from aqueous solution (Tunc et al. 2020) and ciprofloxacin on guava leaves (Tay and Ong 2019).

Pseudo–first (Eq. (6)) and –second-order (Simonin 2016) (Eq. (7)) equations (linear forms) were selected to fit the experimental kinetic data.

$$\log\left(Q_e - Q_t\right) = \log\left(Q_e\right) - \left(\frac{k_1}{2.303}\right)t \quad (6)$$

$$\frac{t}{Q_t} = \frac{1}{k_2 Q_e^{\,2}} + \left(\frac{1}{Q_e}\right)t \quad (7)$$

where k_1 (min^{-1}) and k_2 ($g\ mg^{-1}\ min^{-1}$) are the rate constants for the pseudo-first and –second-order kinetic equation, respectively.

Table 3 presents the kinetic parameters resulting from the fitting. Fig. 7a shows the plot of linearization of the pseudo-first-order model (Tay and Ong 2019), where the slope ($-k_1/2.303$) and intercept $\log(Q_e)$ of plot $\log(Q_e - Q_t)$ versus t were used to determine the pseudo-first-order constant k_1 and the equilibrium adsorption density $Q_{e,cal}$.

Table 3
Kinetic constants for the adsorption of GAT (C0=30 mg/L).

Table 3. Kinetic constants for the adsorption of GAT (C_0 = 30 mg/L).

		Pseudo–first-order model			Pseudo–second-order model		
	$Q_{e,exp}$	k_1	$Q_{e,cal}$	R^2	k_2	$Q_{e,cal}$	R^2
Adsorbent	**(mg/g)**	**(min^{-1})**	**(mg/g)**		**($g\ mg^{-1}\ min^{-1}$)**	**(mg/g)**	
AWC	12.68	0.0298	12.96	0.952	7.8×10^{-5}	38.62	0.886
CAW	12.93	0.0269	10.95	0.964	8.2×10^{-5}	37.31	0.874
WAC	12.95	0.0296	13.00	0.971	5.3×10^{-5}	44.92	0.818

There is a good agreement of experimental data with this model. The obtained correlation coefficients (R^2) were in the range of 0.952–0.971. Also, the adsorption equilibrium values ($Q_{e,cal}$) follow the experimental values. In the case of AWC, the difference was 0.28 mg/g ($Q_{e,cal}$= 12.96 mg/g and $Q_{e,exp}$= 12.68 mg/g), while for other samples the deviation was also very small (CAW: $Q_{e,cal}$= 10.95 mg/g and $Q_{e,exp}$= 12.93 mg/g; WAC: $Q_{e,cal}$= 13.00 mg/g and $Q_{e,exp}$= 12.95 mg/g). These findings suggest that this adsorption system belongs to the pseudo-first-order reaction.

Furthermore, the experimental data fitted the pseudo-second-order equation (Fig. 7b), calculating the respective parameters (Simonin 2016). The slope ($1/Q_e$) and intercept ($1/k_2Q_e^2$) of the plot (t/Q_t) versus t were used to calculate the parameters of k_2 and $Q_{e,cal}$. The straight lines in plots of Fig. 8b showed an unsuccessful fitting with smaller correlation coefficients than those of the pseudo-first-order model. The correlation coefficients was in the range 0.818–0.876, with big differences of the calculated $Q_{e,cal}$ values compared to the experimental ones (AWC: $Q_{e,cal}$ = 12.68 mg/g and $Q_{e,exp}$ = 38.62 mg/g; CAW: $Q_{e,cal}$ = 10.95 mg/g and $Q_{e,exp}$ = 37.31 mg/g; WAC: $Q_{e,cal}$ = 13.00 mg/g and $Q_{e,exp}$ = 44.92 mg/g).

4. Conclusions

The adsorbents were successfully synthesized by using chitosan almond and walnut shells. The prepared beads have advantages because of their biodegradability, low cost, and ease of synthesis. The characterization of beads suggests that hybrid beads are suitable for the adsorption process. Reaction conditions such as pH, dosage, initial concentration and time have greatly influenced adsorption studies. The highest adsorption was attained at pH 5 on CAW beads and pH 7 on AWC and WAC beads. The optimal contact time for equilibrium studies was 120 min for all types of beads. The adsorption isotherms data in AWC beads fit well with the Langmuir model and Freundlich adsorption for CAW and WAC beads. The rate of adsorption on beads follows Lagergren pseudo-second-order kinetics. The results showed that prepared beads could be low-cost for wastewater treatment.

Declarations

Ethical Approval: Here by consciously assure that for the manuscript the following is fulfilled:

1) This material is original work, which has not been previously published elsewhere.

2) The paper is not currently being considered for publication elsewhere.

3) The paper reflects own research and analysis in a truthful and complete manner.

4) The paper properly credits the meaningful contributions of co-authors and co-researchers.

5) The results are appropriately placed in the context of prior and existing research.

6) All sources used are properly disclosed.

7) All authors have been personally and actively involved in substantial work leading to the paper, and will take public responsibility for its content.

Disclosure of potential conflicts of interest: All authors declare that they have no conflicts of interest.

Research involving Human Participants and/or Animals: There was no involvement of Human Participants and/or Animals in the research.

Consent to Participate: Informed consent was obtained from all individual participants included in the study.

Authors Contributions:

Aijaz Ahmad Mala: Material preparation, Basic research, data collection & analysis and base manuscript preparation.

Joydeep Dutta: Analysis, Manuscript checking, editing, Language establishment.

George Z. Kyzas: Data interpretation, analysis, calculation and graphical presentations.

All authors read and approved the final manuscript.

Funding: "The authors declare that no funds, grants, or other support were received during the preparation of this manuscript."

Competing Interest: "The authors have no relevant financial or non-financial interests to disclose."

Availability of data and materials: Derived data supporting the findings of this study are available from the corresponding author on request.

References

1. Ahmad A, Dutta J (2018) Ecotoxicological studies of cephalosporin antibiotics on *Daphnia magna*. Toxicol. Int, 25: 21-30.
2. Ahmad A, Dutta J (2020) The role of combination beads for effective removal of antibiotic cefixime from water: towards of better solution. Journal of Physics: Conference Series 1531:012092. https://doi.org/10.1088/1742-6596/1531/1/012092
3. Ahmed MJ, Theydan SK (2014) Fluoroquinolones antibiotics adsorption onto microporous activated carbon from lignocellulosic biomass by microwave pyrolysis. Journal of the Taiwan Institute of Chemical Engineers 45:219–226. https://doi.org/10.1016/j.jtice.2013.05.014
4. Ahsan MdA, Islam MdT, Hernandez C, et al (2018) Biomass conversion of saw dust to a functionalized carbonaceous materials for the removal of Tetracycline, Sulfamethoxazole and Bisphenol A from water. Journal of Environmental Chemical Engineering 6:4329–4338. https://doi.org/10.1016/j.jece.2018.06.040
5. Amin AS, El-Fetouh Gouda AA, El-Sheikh R, Zahran F (2007) Spectrophotometric determination of gatifloxacin in pure form and in pharmaceutical formulation. Spectrochimica Acta Part A: Molecular and Biomolecular Spectroscopy 67:1306–1312. https://doi.org/10.1016/j.saa.2006.09.041
6. Amouzgar P, Salamatinia B (2015) A short review on presence of pharmaceuticals in water bodies and the potential of chitosan and chitosan derivatives for elimination of pharmaceuticals. J. Mol. Genet. Med, 4(001).
7. Azarpira H, Balarak D (2016) Rice husk as a biosorbent for antibiotic Metronidazole removal: Isotherm studies and model validation - savehums. Savehumsacir. https://doi.org/http://eprints.savehums.ac.ir/13/1/Rice%20husk%20as%20a%20biosorbent%20for%20antibiotic%20Metronidazole%20removal%20Isothe
8. Bajpai S, Bajpai M, Rai N (2012) Sorptive removal of ciprofloxacin hydrochloride from simulated wastewater using sawdust: Kinetic study and effect of pH. Water SA 38: https://doi.org/10.4314/wsa.v38i5.4
9. Balarak D, Azarpira H, Mostafapour, Ferdos Kord (2016) Study of the Adsorption Mechanisms of Cephalexin on to Azolla Filiculoides - savehums. Savehumsacir. https://doi.org/http://eprints.savehums.ac.ir/172/1/2016%208.Azarpira.pdf
10. Carlesi Jara C, Fino D, Specchia V, et al (2007) Electrochemical removal of antibiotics from wastewaters. Applied Catalysis B: Environmental 70:479–487. https://doi.org/10.1016/j.apcatb.2005.11.035
11. Chao S-J, Chung K-H, Lai Y-F, et al (2021) Keratin particles generated from rapid hydrolysis of waste feathers with green DES/KOH: Efficient adsorption of fluoroquinolone antibiotic and its reuse. International Journal of Biological Macromolecules 173:211–218.

https://doi.org/10.1016/j.ijbiomac.2021.01.126

12. Chao Y, Zhu W, Chen J, Wu P, Wu X, Li H, ... Yan S (2014) Development of novel graphene-like layered hexagonal boron nitride for adsorptive removal of antibiotic gatifloxacin from aqueous solution. Green Chemistry Letters and Reviews, 7(4): 330-336.
13. Chayid MA, Ahmed MJ (2015) Amoxicillin adsorption on microwave prepared activated carbon from Arundo donax Linn: Isotherms, kinetics, and thermodynamics studies. Journal of Environmental Chemical Engineering 3:1592–1601. https://doi.org/10.1016/j.jece.2015.05.021
14. Chen Y, Wang F, Duan L, et al (2016) Tetracycline adsorption onto rice husk ash, an agricultural waste: Its kinetic and thermodynamic studies. Journal of Molecular Liquids 222:487–494. https://doi.org/10.1016/j.molliq.2016.07.090
15. Chen Z, Fu J, Wang M, et al (2014) Adsorption of cationic dye (methylene blue) from aqueous solution using poly(cyclotriphosphazene-co-4,4'-sulfonyldiphenol) nanospheres. Applied Surface Science 289:495–501. https://doi.org/10.1016/j.apsusc.2013.11.022
16. Cheng M, Zeng G, Huang D, et al (2016) Hydroxyl radicals based advanced oxidation processes (AOPs) for remediation of soils contaminated with organic compounds: A review. Chemical Engineering Journal 284:582–598. https://doi.org/10.1016/j.cej.2015.09.001
17. Crini G, Badot P-M (2008) Application of chitosan, a natural aminopolysaccharide, for dye removal from aqueous solutions by adsorption processes using batch studies: A review of recent literature. Progress in Polymer Science 33:399–447. https://doi.org/10.1016/j.progpolymsci.2007.11.001
18. Danalıoğlu ST, Bayazit ŞS, Kerkez Kuyumcu Ö, Salam MA (2017) Efficient removal of antibiotics by a novel magnetic adsorbent: Magnetic activated carbon/chitosan (MACC) nanocomposite. Journal of Molecular Liquids 240:589–596. https://doi.org/10.1016/j.molliq.2017.05.131
19. De Gisi S, Lofrano G, Grassi M, Notarnicola M (2015) An overview of low-cost adsorbents for wastewater treatment. Sustainable Materials and Technologies, 9:10.
20. Deng H, Lu J, Li G, et al (2011) Adsorption of methylene blue on adsorbent materials produced from cotton stalk. Chemical Engineering Journal 172:326–334. https://doi.org/10.1016/j.cej.2011.06.013
21. Dorival-García N, Zafra-Gómez A, Navalón A, et al (2013) Removal and degradation characteristics of quinolone antibiotics in laboratory-scale activated sludge reactors under aerobic, nitrifying and anoxic conditions. Journal of Environmental Management 120:75–83. https://doi.org/10.1016/j.jenvman.2013.02.007
22. Du Z, Deng S, Bei Y, et al (2014) Adsorption behavior and mechanism of perfluorinated compounds on various adsorbents—A review. Journal of Hazardous Materials 274:443–454. https://doi.org/10.1016/j.jhazmat.2014.04.038
23. El-Shafey E-SI, Al-Lawati H, Al-Sumri AS (2012) Ciprofloxacin adsorption from aqueous solution onto chemically prepared carbon from date palm leaflets. Journal of Environmental Sciences 24:1579–1586. https://doi.org/10.1016/s1001-0742(11)60949-2
24. Fan S, Wang Y, Li Y, et al (2018) Removal of tetracycline from aqueous solution by biochar derived from rice straw. Environmental Science and Pollution Research 25:29529–29540. https://doi.org/10.1007/s11356-018-2976-0
25. Feng D, Yu H, Deng H, et al (2015) Adsorption Characteristics of Norfloxacin by Biochar Prepared by Cassava Dreg: Kinetics, Isotherms, and Thermodynamic Analysis. BioResources 10:6751–6768
26. Feng Y, Liu Q, Yu Y, et al (2018) Norfloxacin removal from aqueous solution using biochar derived from*luffa*sponge. Journal of Water Supply: Research and Technology-Aqua 67:703–714. https://doi.org/10.2166/aqua.2018.040
27. Filipkowska U, Jóźwiak T (2013) Application of chemically-cross-linked chitosan for the removal of Reactive Black 5 and Reactive Yellow 84 dyes from aqueous solutions. Journal of Polymer Engineering 33:735–747. https://doi.org/10.1515/polyeng-2013-0166
28. Flores-Cano JV, Sánchez-Polo M, Messoud J, et al (2016) Overall adsorption rate of metronidazole, dimetridazole and diatrizoate on activated carbons prepared from coffee residues and almond shells. Journal of Environmental Management 169:116–125. https://doi.org/10.1016/j.jenvman.2015.12.001
29. Fu Y, Yang Z, Xia Y, Xing Y, Gui X (2021) Adsorption of ciprofloxacin pollutants in aqueous solution using modified waste grapefruit peel. Energy Sources, Part A: Recovery, Utilization, and Environmental Effects, 43(2):225-234.
30. García-Galán MJ, Anfruns A, Gonzalez-Olmos R, et al (2016) Advanced oxidation of the antibiotic sulfapyridine by UV/H2O2: Characterization of its transformation products and ecotoxicological implications. Chemosphere 147:451–459. https://doi.org/10.1016/j.chemosphere.2015.12.108
31. González-Pleiter M, Gonzalo S, Rodea-Palomares I, et al (2013) Toxicity of five antibiotics and their mixtures towards photosynthetic aquatic organisms: Implications for environmental risk assessment. Water Research 47:2050–2064. https://doi.org/10.1016/j.watres.2013.01.020
32. He K, Soares AD, Adejumo H, et al (2015) Detection of a wide variety of human and veterinary fluoroquinolone antibiotics in municipal wastewater and wastewater-impacted surface water. Journal of Pharmaceutical and Biomedical Analysis 106:136–143. https://doi.org/10.1016/j.jpba.2014.11.020
33. Homem V, Alves A, Santos L (2010) Amoxicillin degradation at ppb levels by Fenton's oxidation using design of experiments. Science of The Total Environment 408:6272–6280. https://doi.org/10.1016/j.scitotenv.2010.08.058
34. Homem V, Alves A, Santos L (2015) ALTERNATIVE APPROACHES FOR AMOXICILLIN REMOVAL FROM WATER–FENTON'S OXIDATION VERSUS SORPTION BY ALMOND SHELL ASHES. Environmental Engineering & Management Journal (EEMJ), 14(10).
35. Jiang W-T, Chang P-H, Wang Y-S, et al (2013) Removal of ciprofloxacin from water by birnessite. Journal of Hazardous Materials 250-251:362–369. https://doi.org/10.1016/j.jhazmat.2013.02.015
36. Kakavandi B, Esrafili A, Mohseni-Bandpi A, et al (2013) Magnetic Fe3O4@C nanoparticles as adsorbents for removal of amoxicillin from aqueous solution. Water Science and Technology 69:147–155. https://doi.org/10.2166/wst.2013.568
37. Khosravi R, Zarei A, Heidari M, et al (2018) Application of ZnO and TiO2 nanoparticles coated onto montmorillonite in the presence of H2O2 for efficient removal of cephalexin from aqueous solutions. Korean Journal of Chemical Engineering 35:1000–1008. https://doi.org/10.1007/s11814-018-0005-0
38. Kumar M, Dosanjh HS, Singh H (2018) Removal of lead and copper metal ions in single and binary systems using biopolymer modified spinel ferrite. Journal of Environmental Chemical Engineering 6:6194–6206. https://doi.org/10.1016/j.jece.2018.09.054

39. Liang C, Zhang X, Feng P, et al (2018) ZIF-67 derived hollow cobalt sulfide as superior adsorbent for effective adsorption removal of ciprofloxacin antibiotics. Chemical Engineering Journal 344:95–104. https://doi.org/10.1016/j.cej.2018.03.064
40. Liu W, Zhang J, Zhang C, Ren L (2011) Sorption of norfloxacin by lotus stalk-based activated carbon and iron-doped activated alumina: Mechanisms, isotherms and kinetics. Chemical Engineering Journal 171:431–438. https://doi.org/10.1016/j.cej.2011.03.099
41. Ma J, Lei Y, Khan MA, et al (2019) Adsorption properties, kinetics & thermodynamics of tetracycline on carboxymethyl-chitosan reformed montmorillonite. International Journal of Biological Macromolecules 124:557–567. https://doi.org/10.1016/j.ijbiomac.2018.11.235
42. Ma Y, Li M, Wu M, et al (2015) Occurrences and regional distributions of 20 antibiotics in water bodies during groundwater recharge. Science of The Total Environment 518-519:498–506. https://doi.org/10.1016/j.scitotenv.2015.02.100
43. Mahmoud ME, El-Ghanam AM, Mohamed RHA, Saad SR (2020) Enhanced adsorption of Levofloxacin and Ceftriaxone antibiotics from water by assembled composite of nanotitanium oxide/chitosan/nano-bentonite. Materials Science and Engineering: C 108:110199. https://doi.org/10.1016/j.msec.2019.110199
44. Mala AA, Dutta J (2019) Acute and chronic toxicity of fluoroquinolone antibiotics through fresh water cladoceron *Daphnia magna*. Indian Journal of Ecology, 46(4): 874-879.
45. Mala AA, Dutta J (2021). Studies on batch adsorption of gemifloxacin using hybrid beads from biomass. Indian Journal of Ecology, 48(1):116-122.
46. Migneault I, Dartiguenave C, Bertrand MJ, Waldron KC (2004) Glutaraldehyde: behavior in aqueous solution, reaction with proteins, and application to enzyme crosslinking. Biotechniques, 37(5):790-802.
47. Moussavi G, Alahabadi A, Yaghmaeian K, Eskandari M (2013) Preparation, characterization and adsorption potential of the NH4Cl-induced activated carbon for the removal of amoxicillin antibiotic from water. Chemical Engineering Journal 217:119–128. https://doi.org/10.1016/j.cej.2012.11.069
48. Nair V, Panigrahy A, Vinu R (2014) Development of novel chitosan–lignin composites for adsorption of dyes and metal ions from wastewater. Chemical Engineering Journal 254:491–502. https://doi.org/10.1016/j.cej.2014.05.045
49. Nazari G, Abolghasemi H, Esmaieli M, Sadeghi Pouya E (2016) Aqueous phase adsorption of cephalexin by walnut shell-based activated carbon: A fixed-bed column study. Applied Surface Science 375:144–153. https://doi.org/10.1016/j.apsusc.2016.03.096
50. Patel M, Kumar R, Kishor K, Mlsna T, Pittman Jr CU, Mohan D (2019) Pharmaceuticals of emerging concern in aquatic systems: chemistry, occurrence, effects, and removal methods. Chemical reviews, 119(6): 3510-3673.
51. Popoola LT (2020) Tetracycline and sulfamethoxazole adsorption onto nanomagnetic walnut shell-rice husk: isotherm, kinetic, mechanistic and thermodynamic studies. International Journal of Environmental Analytical Chemistry, 100(9):1021-1043.
52. Putra EK, Pranowo R, Sunarso J, et al (2009) Performance of activated carbon and bentonite for adsorption of amoxicillin from wastewater: Mechanisms, isotherms and kinetics. Water Research 43:2419–2430. https://doi.org/10.1016/j.watres.2009.02.039
53. Rathod M, Haldar S, Basha S (2015) Nanocrystalline cellulose for removal of tetracycline hydrochloride from water via biosorption: Equilibrium, kinetic and thermodynamic studies. Ecological Engineering 84:240–249. https://doi.org/10.1016/j.ecoleng.2015.09.031
54. Seo S, Lee K, Min M, et al (2017) A molecular approach to an electrocatalytic hydrogen evolution reaction on single-layer graphene. Nanoscale 9:3969–3979. https://doi.org/10.1039/c6nr09428g
55. Shen R, Yu Y, Lan R, et al (2019) The cardiovascular toxicity induced by high doses of gatifloxacin and ciprofloxacin in zebrafish. Environmental Pollution 254:112861. https://doi.org/10.1016/j.envpol.2019.07.029
56. Simonin J-P (2016) On the comparison of pseudo-first order and pseudo-second order rate laws in the modeling of adsorption kinetics. Chemical Engineering Journal 300:254–263. https://doi.org/10.1016/j.cej.2016.04.079
57. Soares SF, Fernandes T, Trindade T, Daniel-da-Silva AL (2019) Trimethyl Chitosan/Siloxane-Hybrid Coated Fe3O4 Nanoparticles for the Uptake of Sulfamethoxazole from Water. Molecules 24:1958. https://doi.org/10.3390/molecules24101958
58. Tanoue R, Nomiyama K, Nakamura H, Kim JW, Isobe T, Shinohara R, ... Tanabe S (2015) Uptake and tissue distribution of pharmaceuticals and personal care products in wild fish from treated-wastewater-impacted streams. Environmental science & technology, 49(19): 11649-11658.
59. Tay C-I, Ong S-T (2019) Guava Leaves as Adsorbent for the Removal of Emerging Pollutant: Ciprofloxacin from Aqueous Solution. Journal of Physical Science 30:137–156. https://doi.org/10.21315/jps2019.30.2.8
60. Teglia CM, Perez FA, Michlig N, et al (2019) Occurrence, Distribution, and Ecological Risk of Fluoroquinolones in Rivers and Wastewaters. Environmental Toxicology and Chemistry 38:2305–2313. https://doi.org/10.1002/etc.4532
61. Tunç MS, Hanay Ö, Yıldız B (2020) Adsorption of chlortetracycline from aqueous solution by chitin. Chemical Engineering Communications, 207(8):1138-1147.
62. Vakili M, Rafatullah M, Salamatinia B, et al (2015) Elimination of reactive blue 4 from aqueous solutions using 3-aminopropyl triethoxysilane modified chitosan beads. Carbohydrate Polymers 132:89–96. https://doi.org/10.1016/j.carbpol.2015.05.080
63. Wan J, Liu L, Ayub KS, et al (2020) Characterization and adsorption performance of biochars derived from three key biomass constituents. Fuel 269:117142. https://doi.org/10.1016/j.fuel.2020.117142
64. Wang N, Xiao W, Niu B, et al (2019) Highly efficient adsorption of fluoroquinolone antibiotics using chitosan derived granular hydrogel with 3D structure. Journal of Molecular Liquids 281:307–314. https://doi.org/10.1016/j.molliq.2019.02.061
65. Wang S, Wang H (2015) Adsorption behavior of antibiotic in soil environment: a critical review. Frontiers of Environmental Science & Engineering 9:565–574. https://doi.org/10.1007/s11783-015-0801-2
66. Xiao Y, Chang H, Jia A, Hu J (2008) Trace analysis of quinolone and fluoroquinolone antibiotics from wastewaters by liquid chromatography–electrospray tandem mass spectrometry. Journal of Chromatography A 1214:100–108. https://doi.org/10.1016/j.chroma.2008.10.090

67. Xie A, Dai J, Chen X, et al (2016) Hierarchical porous carbon materials derived from a waste paper towel with ultrafast and ultrahigh performance for adsorption of tetracycline. RSC Advances 6:72985–72998. https://doi.org/10.1039/c6ra17286e
68. Xiong J-Q, Kurade MB, Jeon B-H (2017) Biodegradation of levofloxacin by an acclimated freshwater microalga, Chlorella vulgaris. Chemical Engineering Journal 313:1251–1257. https://doi.org/10.1016/j.cej.2016.11.017
69. Xuemin L, Yinan L, Jianxiu H, Weihong W (2018) Study of Almond Shell Characteristics, Materials. 11:1-12.
70. Yadav S, Goel N, Kumar V, et al (2017) Removal of fluoroquinolone from aqueous solution using graphene oxide: experimental and computational elucidation. Environmental Science and Pollution Research 25:2942–2957. https://doi.org/10.1007/s11356-017-0596-8
71. Yu F, Li Y, Han S, Ma J (2016) Adsorptive removal of antibiotics from aqueous solution using carbon materials. Chemosphere 153:365–385. https://doi.org/10.1016/j.chemosphere.2016.03.083
72. Yu Y, Zhou Y, Wang Z, et al (2017) Investigation of the removal mechanism of antibiotic ceftazidime by green algae and subsequent microbic impact assessment. Scientific Reports 7: https://doi.org/10.1038/s41598-017-04128-3
73. Zeng ZW, Tan XF, Liu YG, Tian SR, Zeng GM, Jiang LH, ... Yin ZH (2018) Comprehensive adsorption studies of doxycycline and ciprofloxacin antibiotics by biochars prepared at different temperatures. Frontiers in Chemistry, 6: 80.
74. Zhang R, Tang J, Li J, et al (2013) Antibiotics in the offshore waters of the Bohai Sea and the Yellow Sea in China: Occurrence, distribution and ecological risks. Environmental Pollution 174:71–77. https://doi.org/10.1016/j.envpol.2012.11.008
75. Zhao R, Ma T, Zhao S, et al (2020) Uniform and stable immobilization of metal-organic frameworks into chitosan matrix for enhanced tetracycline removal from water. Chemical Engineering Journal 382:122893. https://doi.org/10.1016/j.cej.2019.122893
76. Zheng H, Wang Z, Zhao J, et al (2013) Sorption of antibiotic sulfamethoxazole varies with biochars produced at different temperatures. Environmental Pollution 181:60–67. https://doi.org/10.1016/j.envpol.2013.05.056
77. Zhou C, Lai C, Xu P, Zeng G, Huang D, Li Z, ... Deng R (2018) Rational design of carbon-doped carbon nitride/Bi12O17Cl2 composites: a promising candidate photocatalyst for boosting visible-light-driven photocatalytic degradation of tetracycline. ACS Sustainable Chemistry & Engineering, 6(5): 6941-6949.
78. Zularisam AW, Ismail AF, Salim R (2006) Behaviours of natural organic matter in membrane filtration for surface water treatmnt — a review. Desalination 194:211–231. https://doi.org/10.1016/j.desal.2005.10.030

Figures

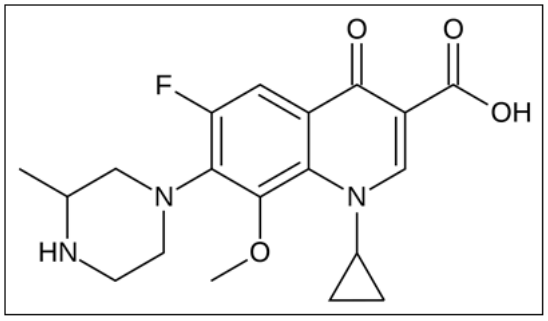

Figure 1

Molecular structure of gatifloxacin

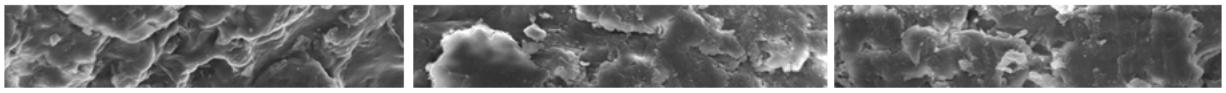

Figure 2

SEM micrograph images of AWC (a-b), CAW (c-d) and WAC beads (e-f).

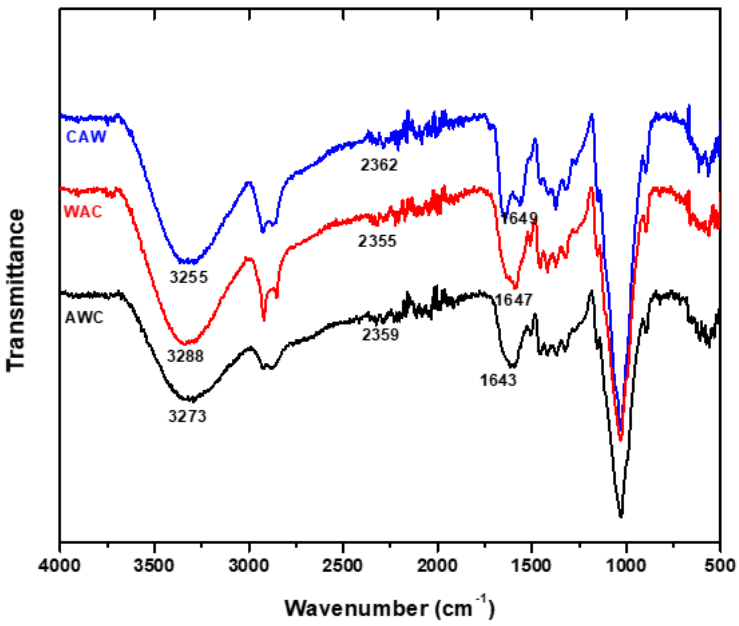

Figure 3

FTIR of (a) AWC, (b) CAW, and (c) WAC before and after adsorption.

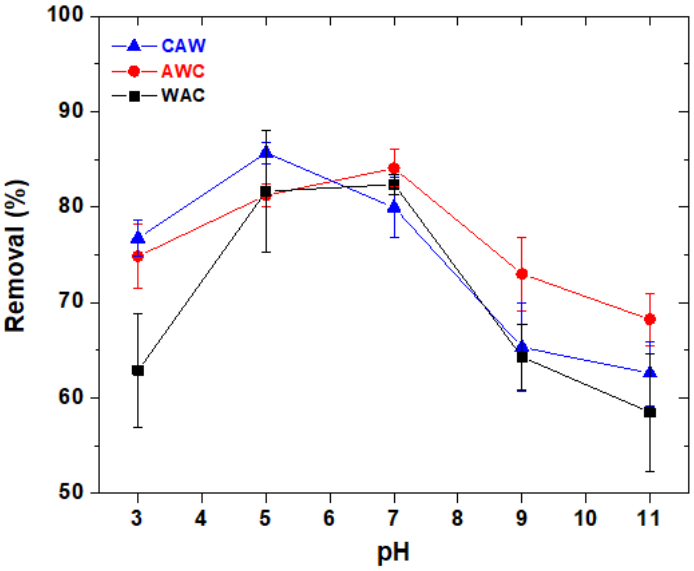

Figure 4

Effect of pH on the removal of gatifloxacin by adsorption onto AWC, CAW and WAC beads (V = 50 mL, m = 0.1g, C_0 = 30 mg/L, N = 150 rpm, T = 30 °C).

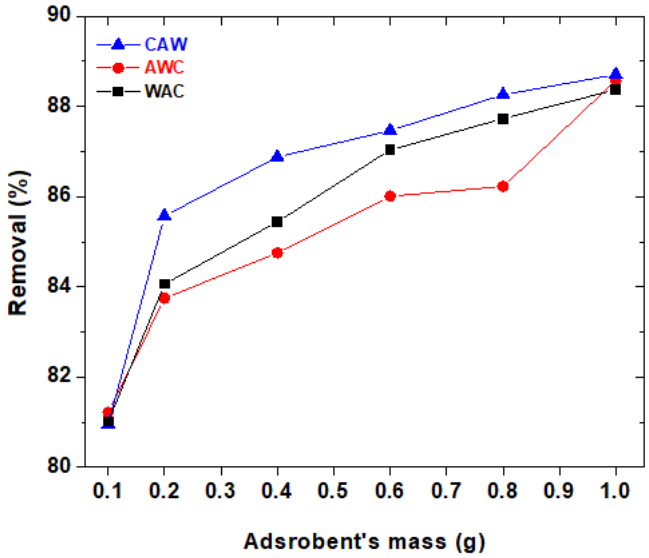

Figure 5

Effect of adsorbent's dosage on the removal of gatifloxacin by adsorption onto AWC, CAW and WAC beads (V = 50 mL, C_0 = 30 mg/L, N = 150 rpm, T = 30 °C).

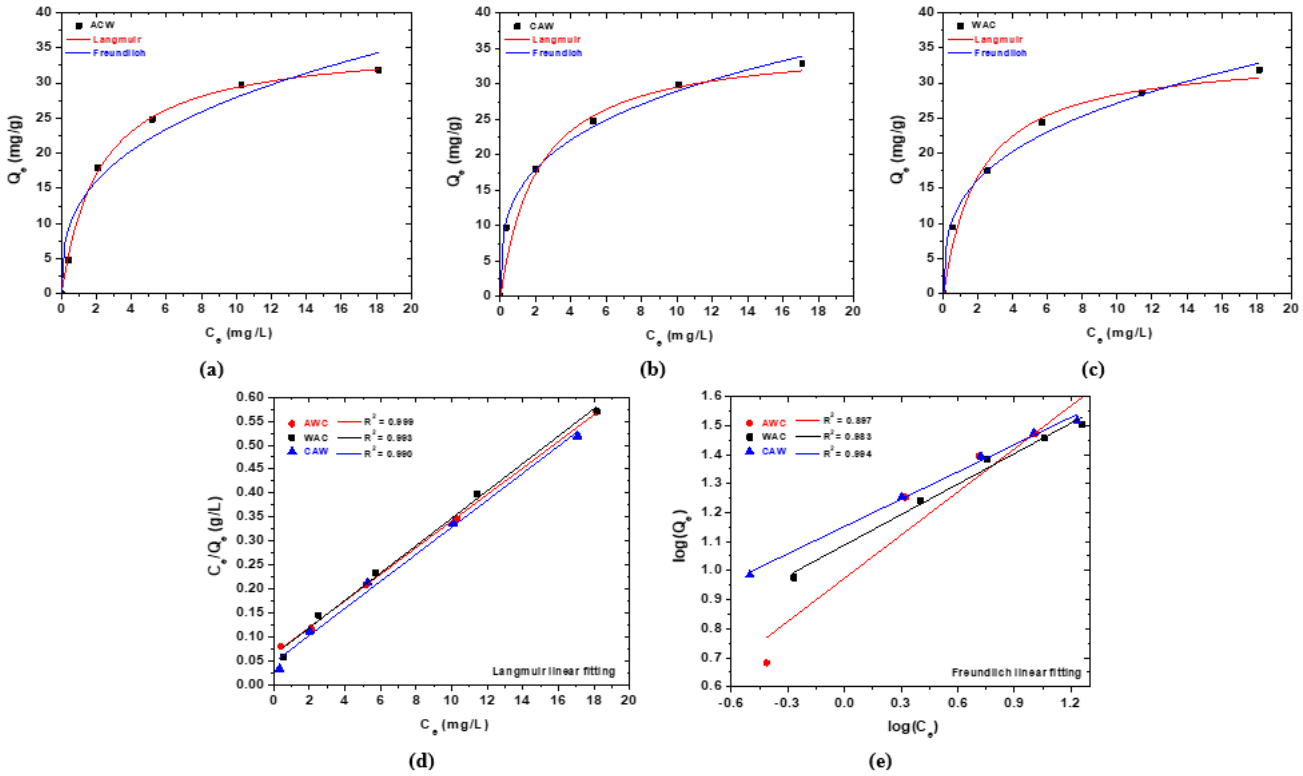

Figure 6

Isotherms (Langmuir and Freundlich) of the adsorption of GAT onto AWL, CAW and WAC beads (V = 50 mL, m =0.1g, N = 150 rpm, T = 30 °C).(a-c) Non-linear fitting, (d-e) Linear fitting.

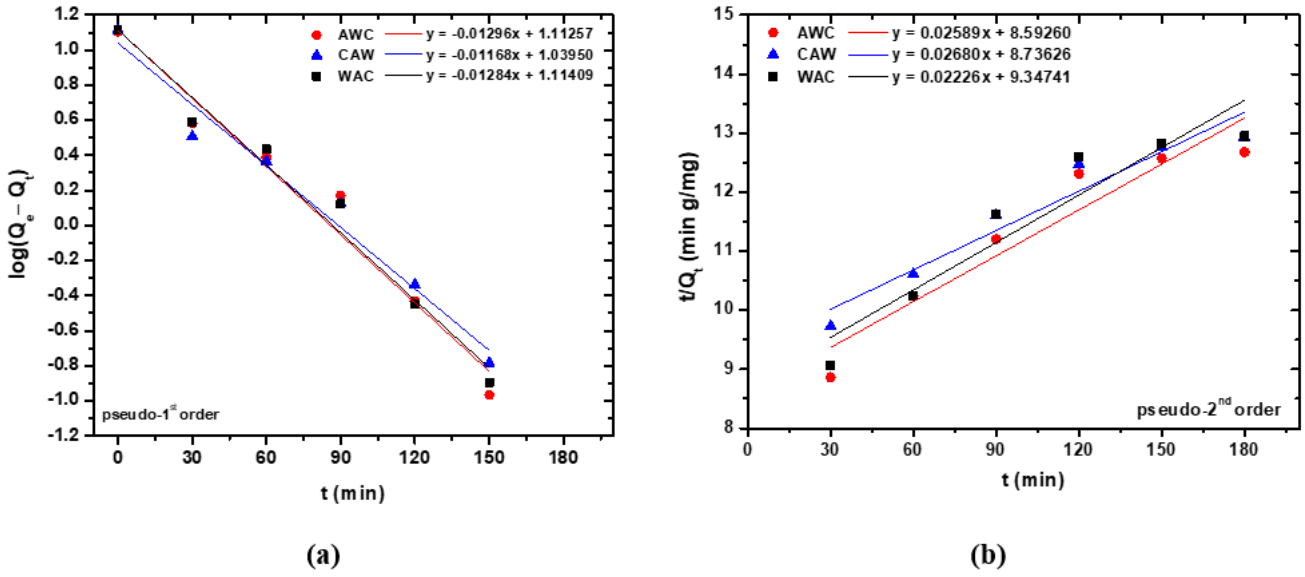

Figure 7

Effect of contact time on the adsorption of gatifloxacin by AWC, CAW and WAC beads (V = 50 mL, m = 0.1g, C_0 = 30 mg/L, N = 150 rpm, T = 30 °C).